

Article

Effect of the Textures and Particle Sizes of Limestone on the Quicklime Reaction Activity

Minjie Zhu ¹, Jing Wu ^{1,*}, Zehao Yang ¹, Yong Zhu ², Quan Rong ² and Qingfu Wen ²

¹ School of Resources, Environment and Materials, Guangxi University, Nanning 530004, China; 2115392106@st.gxu.edu.cn (M.Z.)

² Guangxi Huana New Materials Co., Ltd., Nanning 530100, China

* Correspondence: 20140018@gxu.edu.cn

Abstract: Quicklime is not only an important raw material for the steel and nano-calcium carbonate industries but also a key carrier for capturing carbon dioxide in the fight against global warming, and its reaction activity plays a vital role in these processes. Recent studies have found that quicklime produced from limestones with similar chemical compositions under the same production process has significantly different reaction activities, which indicates that something other than the chemical composition of limestone affects quicklime reaction activity. To explore the factors affecting quicklime reaction activity, this study analyzed the textures and calcite particle size of limestone collected from different areas of Guangxi, China, and measures the quicklime reaction activity with different calcination times. It has been found that: (1) limestone with a clastic texture is preferred to that with a crystalline texture (including transition type) in yielding quicklime with higher reaction activity; and (2) for limestone with a clastic texture, fine-grained limestone tends to produce the same or higher quicklime reaction activity with lower energy consumption.

Keywords: limestone texture; particle size; carbon dioxide capture; quicklime reaction activity



Citation: Zhu, M.; Wu, J.; Yang, Z.; Zhu, Y.; Rong, Q.; Wen, Q. Effect of the Textures and Particle Sizes of Limestone on the Quicklime Reaction Activity. *Minerals* **2023**, *13*, 1201. <https://doi.org/10.3390/min13091201>

Academic Editor: Paulina Faria

Received: 30 July 2023

Revised: 5 September 2023

Accepted: 8 September 2023

Published: 13 September 2023



Copyright: © 2023 by the authors. Licensee MDPI, Basel, Switzerland. This article is an open access article distributed under the terms and conditions of the Creative Commons Attribution (CC BY) license (<https://creativecommons.org/licenses/by/4.0/>).

1. Introduction

Quicklime is a widely used inorganic compound. Quicklime reaction activity plays a crucial role in various industries and applications. To begin with, in traditional industries such as iron and steel production and infrastructure construction, quicklime is used as a flux in iron smelting furnaces. High-reactivity quicklime helps lower the melting temperature of slag, thereby accelerating the smelting process [1,2]. Quicklime is also commonly used in the manufacturing of lightweight construction materials. High-reactivity quicklime imparts good insulation and thermal properties to these materials [3]. Furthermore, in emerging industries such as nano-calcium carbonate, high-reactivity quicklime facilitates the synthesis of nano-calcium carbonate and improves its performance. Additionally, quicklime is an indispensable component of carbon capture technologies, where high-reactivity quicklime promotes the absorption and reaction of carbon dioxide, thereby reducing greenhouse gas emissions [4–6]. Therefore, quicklime reaction activity is significant for the development of both traditional and emerging industries.

There are many factors affecting quicklime reaction activity. Different limestones can result in different quicklime reaction activities [7]. Limestone with CaO content > 54.5 wt.% and grain size < 0.04 mm is suitable for the production of highly reactive quicklime, whereas dense structural limestone is not favorable for the production of highly reactive quicklime [8–13]. The calcination experiment on limestone shows that the quicklime reaction activity will decrease if the calcination temperature is too high or the time is too long [14–17]. Furthermore, calcium oxide from hydroxide has a higher reaction activity than that from carbonate [18]. The quicklime reaction activity actually depends largely on the porosity and specific surface area of the quicklime itself, which has the highest activity

under high porosity and specific surface area conditions [19–21]. This is because, as the porosity of the limestone increases, the heat from the outside penetrates more evenly into the limestone particles, and the uniformity of the heat increases the quicklime reaction activity [22].

In summary, the predecessors mainly focused on the effect of the limestone chemical composition, calcination time, and temperature on quicklime reaction activity, whereas little research has been conducted on the relationship between the natural physicochemical parameters of limestone and quicklime reaction activity, such as the texture of limestone, the calcite particle size of limestone, etc. To further verify the effect of texture and calcite particle size of limestone on quicklime reaction activity, this study, based on DLT 323-2010 (measurement method for activity of quicklime used in dry flue gas desulfurization) for the determination of quicklime reaction activity, analyzes eleven (11) groups of limestone collected from nine (9) limestone mines in different urban areas of Guangxi Province, China, with the aim of studying the key factors affecting quicklime reaction activity.

2. Sample Collection Principles

The 11 sets of samples were collected from 9 mines in Guangxi, China (Figure 1). The collection of samples was based on the following three principles (Table 1):

- (1) Differences in the location. To better differentiate and understand the effect of the natural physicochemical parameters of limestone on quicklime reaction activity, representative samples from each mine were selected that fully reflect the characteristics of limestone from different locations and different geological environments in Guangxi province, China.
- (2) Similarities of the main chemical compositions. The limestones selected for this research are of high grade (CaO content > 54.0 wt.%, MgO content < 1.0 wt.%).
- (3) Differences in calcite grain size. The differences in calcite grain size of limestone were taken into consideration, and two groups of limestone with obvious differences in calcite grain size were collected.

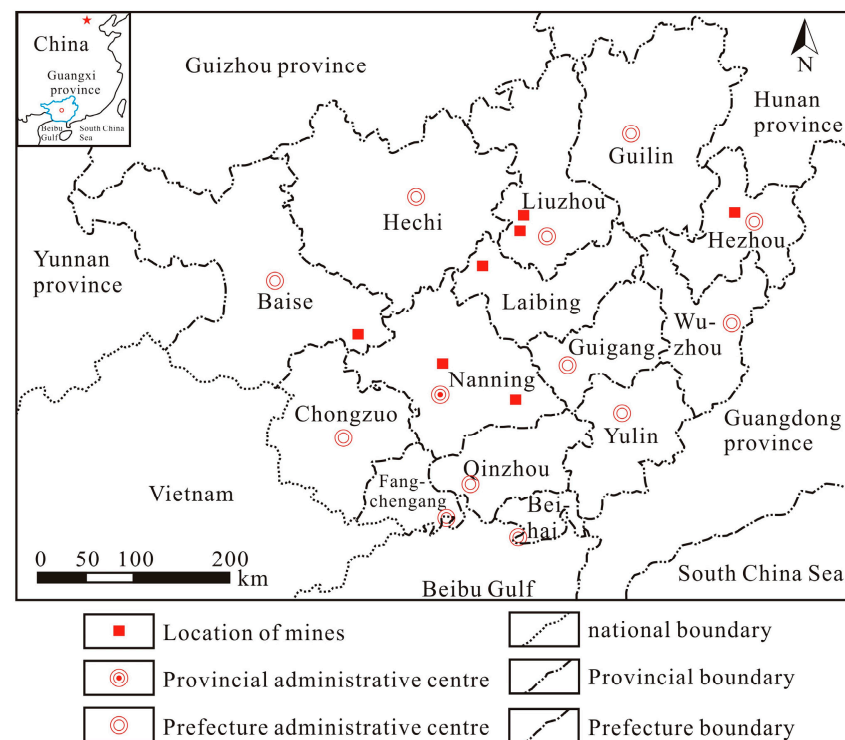


Figure 1. Sample distribution map.

Table 1. Table of major elemental composition and characteristics of limestone.

Serial Number of Mines	Name of the Mines	Mine Codes	Location of Mines	Strata of the Sample	Limestone Major Element Composition		Note
					CaO/wt.%	MgO/wt.%	
1	Mt Mao	MD	Liunan District, Liuzhou, China	Upper Devonian Rongxian Formation (D_{3r})	54.77	0.64	
2	Mt Baiyun	BYS	Liunan District, Liuzhou, China	Middle Carboniferous Huanglong Formation (C_2h)	54.50	0.48	
3	Mt Dadu	DD	Hengzhou, Nanning, China	Upper Carboniferous Huanglong Formation (C_2h)	54.58	0.54	Limestone
4	Mt Longmeng	LMS	Wuming District, Nanning, China	Upper Devonian Tianziling Formation (D_{3t})	55.52	0.20	
5	Mt Pingguo (Coarse-grained)	PGC	Pingguo, Baise, China	Carboniferous Middle Formation Huanglong Group (C_2h)	54.08	0.58	
	Mt Pingguo (Fine-grained)	PGX			55.11	0.68	
6	Mt Shangjiao	SJS	Wuming District, Nanning, China	Upper Devonian Rongxian Formation (D_{3r})	54.58	0.24	
7	Mt Shuma	SM	Wuming District, Nanning, China	Upper Devonian Rongxian Formation (D_{3r})	55.00	0.21	
8	Mt Xingcheng (Coarse-grained)	XCC	Xincheng County, Laibin, China	Carboniferous Nandan Formation (C_2Pn)	54.61	0.79	
	Mt Xingcheng (Fine-grained)	XCX			55.31	0.40	
9	Mt Jiangjun	JJ	Babu District, Hezhou, China	Middle Devonian Tangjiawan Formation (D_2t)	54.71	0.68	Recrystallized calcite

Note: The CaO and MgO contents of the limestone samples were analyzed at the Analysis and Testing Centre of Guangxi Metallurgical Research Institute.

Based on the above three principles, representative samples without late calcite veins or veinlets were selected from 9 mines. A total of 11 groups of limestone samples from different ages, from the Middle Devonian to the Upper Carboniferous, each of 10 to 15 kg, were collected. These limestone samples were carefully cleaned to remove contaminants that might affect subsequent analyses. These 11 groups of limestone samples were processed in three steps. Step 1: Selection of samples without late micro-calcite veins for thin sectioning and microscopic observation; Step 2: Chemical composition analysis; Step 3: Limestone calcination and determination of quicklime reaction activity.

3. Analytical Methods and Results

3.1. Limestone Major Element Composition Analysis

The CaO and MgO composition analysis method used was X-ray fluorescence spectrometry based on YST 703-2014 “Determination of Element Content in Chemical Analysis Methods of Limestone by X-ray Fluorescence Spectrometry”. The experimental instrument was the XRF-1800 wavelength-dispersive X-ray fluorescence spectrometer (Shimadzu Corporation, Kyoto, Japan), and the detection limits of CaO and MgO were 0.10 wt.% and 0.05 wt.%, respectively. The test results are shown in Table 1.

The CaO and MgO contents of the 11 groups of limestone ranged from 54.08 to 55.52 wt.% and from 0.21 to 0.79 wt.%, respectively. All samples were selected in accordance with sample selection principles.

3.2. The Texture of Limestone

The limestone texture observation work was conducted in the Rock and Mineral Laboratory of Guangxi University. By using a Leica DM 2700 polarization microscope, the limestone could be classified into three types based on the observation results: clastic texture, transitional crystalline texture, and crystalline texture.

3.2.1. Clastic Texture

Clastic texture could be further subdivided into oolitic-clastic texture and bioclastic texture.

Oolitic-clastic texture: MD, DD, and SJS are limestones with oolitic-clastic textures (Figure 2). Oolite is a spherical or ellipsoidal particle consisting of a core and an encrustation surrounding the core. The core of the oolite is usually internal debris. The oolitic grains are rounded or oval, accounting for about 60 to 80 vol%. Its diameter ranges from 200 to 600 μm . The cement is mainly bright calcite, which accounts for about 20 to 40 vol%. The size of the bright calcite is 20 to 30 μm . This type of limestone contains 98 to 99 vol% calcites.

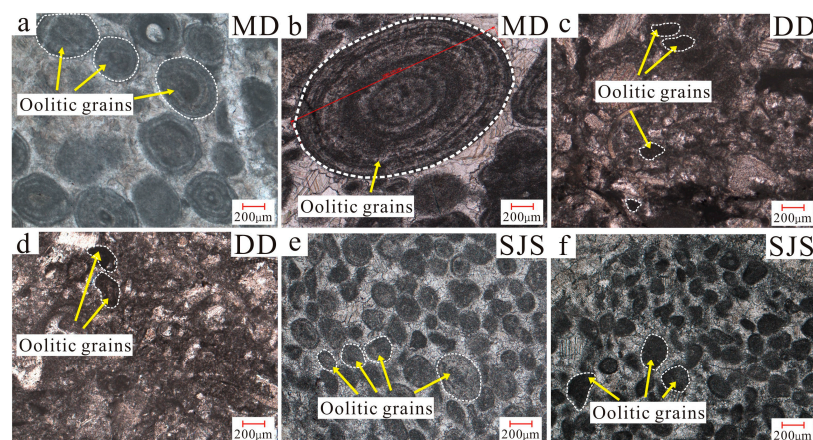


Figure 2. Micrographs of limestone with oolitic-clastic texture from MD, DD, and SJS in Guangxi, China: (a,b) (MD) from the Liunan District, Liuzhou; (c,d) (DD) from the Hengzhou County, Nanning; (e,f) (SJS) from the Wuming District.

Bioclastic texture: PGC, PGX, SM, XCC, and XCX are limestones with a bioclastic texture (Figure 3). The particles are mainly sandy debris and biological debris. Foraminiferal shells with diameters varying from 200 to 1000 μm can be found (Figure 3a,c,g,i). The limestone contains $40 \pm \text{vol}\%$ sandy debris, $30 \pm \text{vol}\%$ biological debris, and $30 \pm \text{vol}\%$ cement. The cement particle size is 10 to 30 μm .

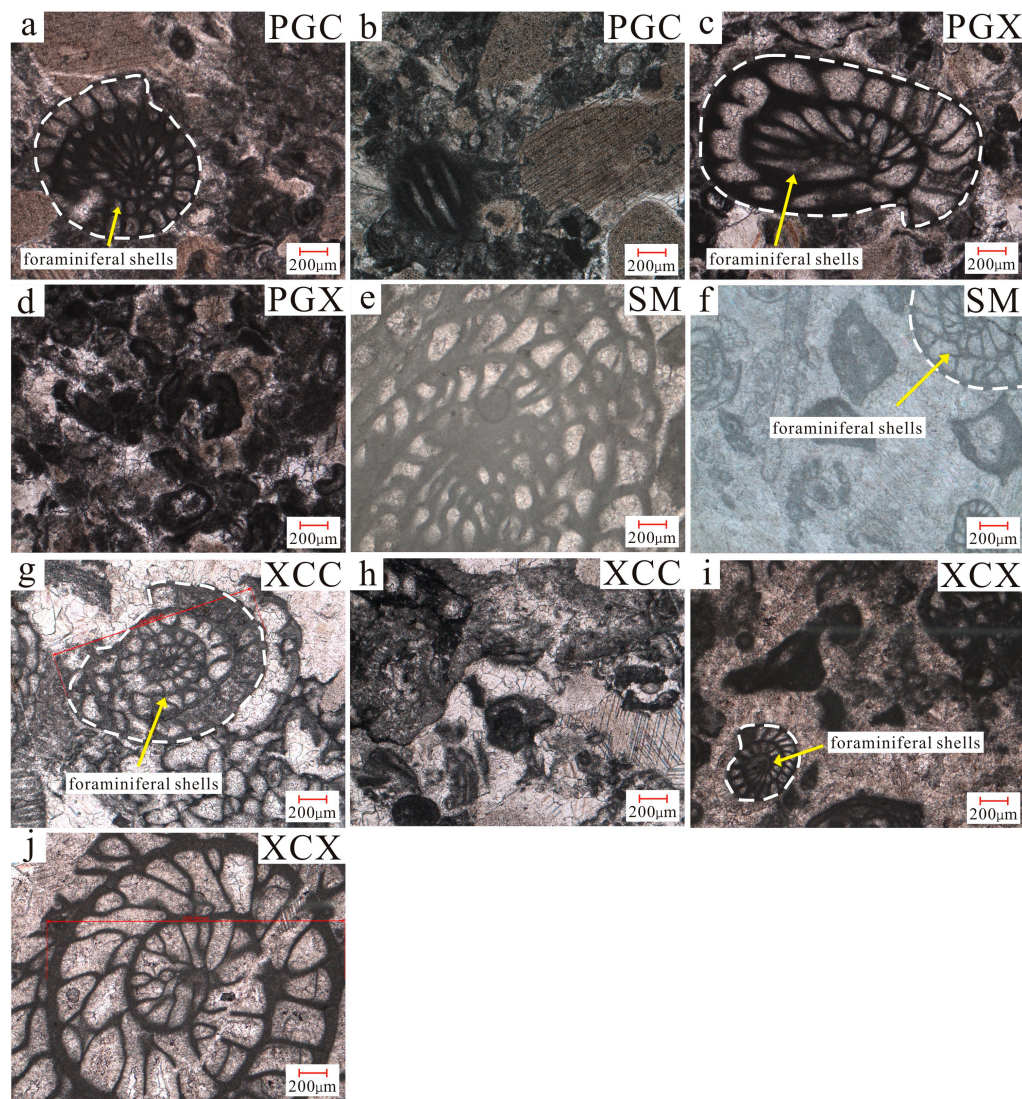


Figure 3. Micrographs of limestone with bioclastic texture from PGC, PGX, SM, XCC, and XCX in Guangxi, China: (a,b) (PGC) limestone with coarse-grained bioclastic texture from the Pingguo County, Baise; (c,d) (PGX) limestone with fine-grained bioclastic texture from Pingguo County, Baise; (e,f) (SM) from the Wuming District; (g,h) (XCC) limestone with coarse-grained bioclastic texture from Xincheng County, Laibin; (i,j) (XCX) limestone with fine-grained bioclastic texture from Xincheng County, Laibin.

3.2.2. Transitional Crystalline Texture

The limestone with transitional crystalline texture (Figure 4) is a type of limestone of whose texture has been completely or partially recrystallized during the late geological events. Most of the calcite in the LMS has been recrystallized, and the former clastic texture can only be found partially (Figure 4a). The recrystallized grains sizes range from 80 to 100 μm .

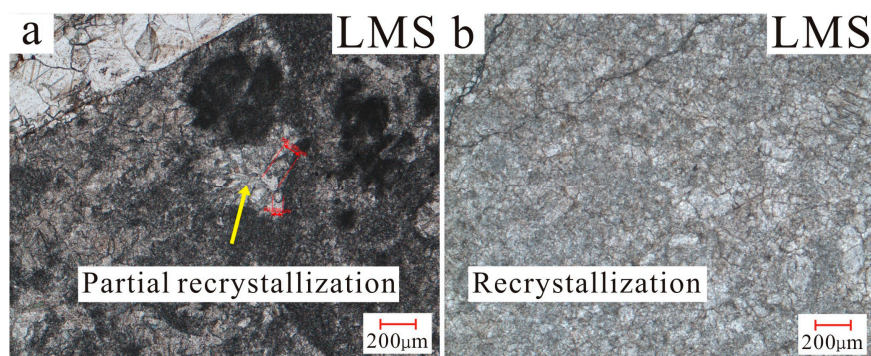


Figure 4. Micrograph of limestone with transitional crystalline texture from LMS in Guangxi, China: (a,b) (LMS) from the Wuming District.

3.2.3. Crystalline Texture

The crystalline texture of limestone can be divided into fine-grained and coarse-grained textures. The limestone with a fine-grained texture is represented by BYS (Figure 5a,b). This type of limestone has an overall equigranular grain size of mainly approximately $0.02\ \mu\text{m}$. The limestone is overall a dark gray color and contains $99 \pm \text{vol}\%$ calcite.

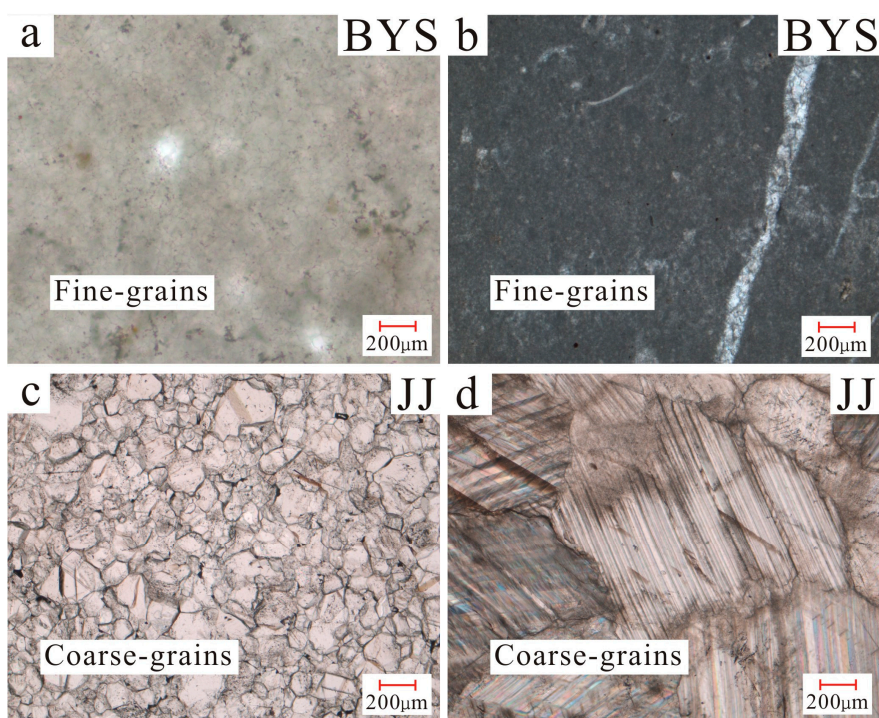


Figure 5. Micrograph of limestone with crystalline texture from BYS and JJ in Guangxi, China: (a,b) (BYS) fine-grained crystalline limestone from the Liunan District, Liuzhou; (c,d) (JJ) coarse-grained crystalline limestone from the Babu District, Hezhou.

The limestone with a coarse-grained texture is represented by JJ (Figure 5c,d). It has a high portion of crystallized calcite, with grain sizes ranging from 100 to $200\ \mu\text{m}$. This type of limestone contains fewer impurities and has a relatively homogeneous texture overall, indicating that such limestone was recrystallized in the late geological event.

3.3. Calcite Particle Size with Clastic Texture

The limestone with clastic texture from Pingguo and Xincheng mines contains calcite grains of different sizes (Table 2). Based on microscopic observations, the particle size distribution was roughly estimated. The limestone with over 50% calcite particles of a

size greater than 5 μm was defined as coarse-grained limestone, and the limestone with over 50% calcite particles of a size less than or equal to 5 μm was defined as fine-grained limestone. The average calcite grain sizes of coarse-grained and fine-grained limestone from the Pingguo mine are 7 μm and 5 μm , respectively. The average calcite grain sizes of coarse-grained and fine-grained limestone from the Xincheng mine are 10 μm and 4 μm , respectively. The average calcite grain size of the two Pingguo limestone samples is 6 μm and the average calcite grain size of the two Xincheng limestone samples is 7 μm . The average calcite grain size of the limestone from the Xincheng mine is 17% larger than that from the Pingguo mine.

Table 2. Grain size statistics for calcites of limestone with clastic texture.

Serial Number of the Group	Mine Names	Mine Codes	The Calcite Particle Size of Internal Debris/ μm	Percentage of Gradation of Particle Size/%	Average Particle Size/ μm
1	Mt Pingguo (coarse-grained)	PGC	2–5	10	6
			5–10	50	
			>10	40	
	Mt Pingguo (fine-grained)	PGX	2–5	70	5
			5–10	20	
			>10	10	
2	Mt Xincheng (coarse-grained)	XCC	2–5	20	10
			5–10	60	
			>10	20	
	Mt Xingcheng (fine-grained)	XCX	2–5	50	4
			5–10	40	
			>10	10	

3.4. Determination of Quicklime Reaction Activity

Quicklime reaction activity is the time needed to test the temperature of the reaction solution from 20 °C to 60 °C during the digestion reaction between quicklime and deionized water. The shorter the time required for the reaction, the higher the quicklime reaction activity, and vice versa.

The determination of quicklime reaction activity was carried out in the chemistry laboratory of Guangxi Huana New Materials Co., Ltd (Nanning, China). The experimental equipment and reagents, including an MF-1700CIII high-temperature chamber furnace (mainly used for calcining limestone) (Anhui BEQ Equipment Technology Co., Ltd., Hefei, China), a Dewar vessel, a magnetic stirrer, a thermocouple thermometer, a timer, a cooling ice bag, and deionized water, were used.

The apparent calcite fine-veined samples were removed at first, and 11 groups of limestone samples were crushed into 2-cm-sized gravel pieces. The reaction activity, according to EN 459-2, was high for lime burned at 1050 °C. Moreover, because there are too many variables affecting quicklime reaction activity, some related studies have also studied the effect of calcination temperature on quicklime reaction activity [23–25]. Therefore, this study focused on the effect of calcination time and calcite particle size on quicklime reaction activity. The calcination temperature was set to be a constant 1050 °C, and the calcination time was set to be 4 h, 5 h (BYS samples were set to 4 h, 5 h, and 6 h). Crushed limestone gravel pieces weighing 1000 ± 1 g were placed in the furnace for 4 h and 5 h, respectively, at a temperature of 1050 °C. The quicklime reaction activity produced by calcining BYS limestone for 4 h was not able to reach the lower limit of the assay, so the calcination time of the BYS limestone sample was increased to 6 h. The limestone samples were calcined to produce quicklime, which was later ground into powder and then screened out through a 100-mesh screen (0.150 mm). Then, deionized water and cooling ice bags were added to the Dewar vessel. The cooling ice bags were used to reduce the

temperature of the deionized water to 20 °C, and quicklime powder was added to the Dewar vessel for the reaction. During this process, the magnetic stirrer was used to make the lime and water fully reactive. The time needed to test the temperature of the reaction solution from 20 °C to 60 °C, which is the quicklime reaction activity T60, was recorded.

The quicklime reaction activity T60 for each group of limestone samples after calcination with different time periods is shown in Table 3 and Figure 6.

Table 3. The reaction activity T60 statistics for each quicklime sample.

Serial Number of Mines	Name of the Mines	Mine Codes	Calcination Time of Limestone/h	The Quicklime Reaction Activity T60/s
1	Mt Mao	MD	4	26.0
			5	48.0
2	Mt Baiyun	BYS	4	/
			5	152.0
			6	61.0
3	Mt Baiyun	DD	4	26.0
			5	19.0
4	Mt Longmeng	LMS	4	98.0
			5	76.0
5	Mt Pingguo (Coarse-grained)	PGC	4	21.0
			5	24.0
6	Mt Pingguo (Fine-grained)	PGX	4	18.0
			5	28.0
7	Mt Shangjiao	SJS	4	24.0
			5	19.0
8	Mt Shuma	SM	4	39.0
			5	26.0
9	Mt Pingguo (Coarse-grained)	XCC	4	29.0
			5	16.0
10	Mt Pingguo (Fine-grained)	XCX	4	28.0
			5	35.0
11	Mt Jiangjun	JJ	4	33.0
			5	36.0

Note: “/” indicates that the reaction solution temperature could not reach 60 °C.

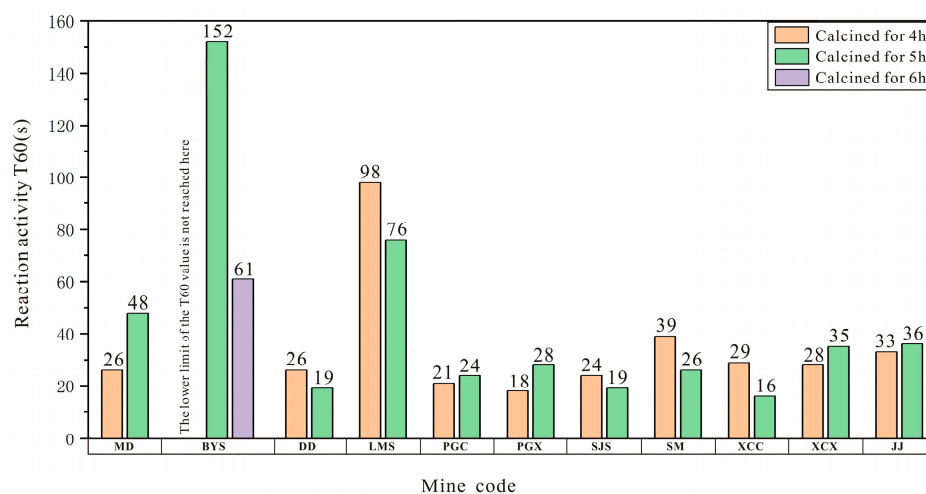


Figure 6. Histogram of the quicklime reaction activity T60 of different samples.

The T60 values of the quicklime samples ranged from 18.0 to 98.0 s under 4 h of calcination (Figure 6), with an average T60 value of approximately 31.0 s. The T60 values of LMS (98.0 s) and SM (39.0 s) were higher than the average value, indicating its relative reaction activity was comparatively low. The T60 value of the PGX was 18.0 s, indicating its reaction activity was the highest among all the tested samples. The reaction solution temperature formed by the BYS quicklime reaction with water could not reach 60 °C, indicating its lowest reaction activity.

The T60 values for all quicklime samples ranged from 16.0 to 152.0 s under 5 h of calcination, with an average T60 value of approximately 43.5 s. The T60 values of BYS (152.0 s), LMS (76.0 s), and MD (48.0 s) were all higher than the average values. The T60 value of the XCC was 16.0 s, indicating its highest reaction activity among all the tested samples. The T60 value of the BYS is 152.0 s, indicating its lowest reaction activity among all the tested samples.

The T60 value of the BYS under 6 h of calcination was 61.0 s. This value is still higher than the average level under 4 h and 5 h calcination, indicating its comparatively low reaction activity.

4. Discussion

4.1. The Effect of Limestone Texture on Quicklime Reaction Activity

The texture of limestone is mainly classified into three types: clastic texture, transitional crystalline texture, and crystalline texture (Table 4). The relationship between the quicklime reaction activity and the three textural types of limestone is shown in Figures 7 and 8.

Table 4. Relation between limestone texture and quicklime reaction activity T60.

Serial Number of Mines	Names of the Mines	Mine Codes	Primary Texture	Secondary Texture	The Quicklime Reaction Activity T60 under Different Calcination Time/s		
					Calcined for 4 h	Calcined for 5 h	Calcined for 6 h
1	Mt Mao	MD	Clastic texture	Clastic-oolitic-texture	26.0	48.0	-
2	Mt Dadu	DD			26.0	19.0	-
3	Mt Shangjiao	SJS			24.0	19.0	-
4	Mt Pingguo (Coarse-grained)	PGC	Clastic texture	Bioclastic texture	21.0	24.0	-
	Mt Pingguo (Fine-grained)	PGX			18.0	28.0	-
5	Mt Shuma	SM			39.0	26.0	-
6	Mt Xincheng (Coarse-grained)	XCC			29.0	16.0	-
	Mt Xincheng (Fine-grained)	XCX			28.0	35.0	-
7	Mt Longmeng	LMS			Transitional crystalline texture	-	98.0
8	Mt Baiyun	BYS	Crystalline texture	Fine-grained texture	/	152.0	61.0
9	Mt Jiangjun	JJ		Coarse-grained texture	33.0	36.0	

Note: "/" indicates that the reaction solution temperature could not reach 60 °C.

The T60 values of the MD and PGX samples were 26.0 s and 18.0 s under 4 h of calcination, respectively, and 48.0 s and 28.0 s under 5 h of calcination, respectively (Figures 7 and 8). With an increase in calcination time, the T60 values of samples MD and PGX increased significantly, indicating that the quicklime reaction activity decreased significantly. This phenomenon can be explained as "over-burnt". It means that too high a calcination temperature or too long a calcination time can lead to calcium oxide particles sintering together, resulting in a reduction in porosity and then a decrease in quicklime

reaction activity [26]. The T60 values of the SM and XCC samples were 39.0 s and 29.0 s under 4 h of calcination, and 26.0 s and 16.0 s under 5 h of calcination, respectively. With an increase in calcination time, the T60 values of samples SM and XCC decreased significantly, indicating that the quicklime reaction activity increased significantly. This phenomenon can be explained as “under-burnt”. It means that the calcium carbonate was not completely decomposed. It can be concluded that calcination time has a substantial impact on quicklime reaction activity, and such a conclusion is consistent with the previous research. The combination of optimal calcination temperature and time duration yielded high quicklime reaction activity, whereas excessively high or low temperatures as well as excessively long or short calcination times possibly diminished quicklime reaction activity [27–30].

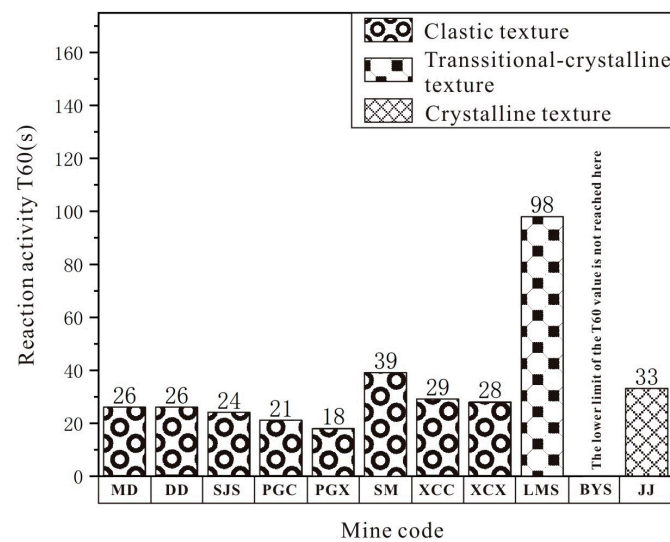


Figure 7. Histogram shows the limestone texture and quicklime reaction activity T60 for limestone under 4 h of calcination.

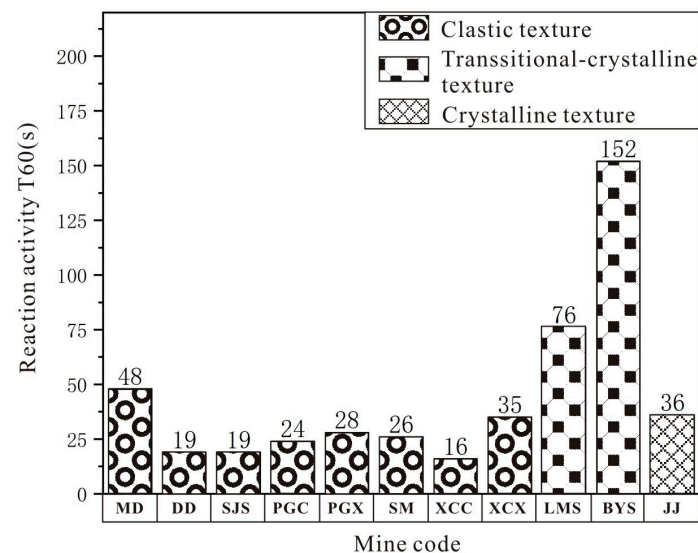


Figure 8. Histogram shows the limestone texture and quicklime reaction activity T60 for limestone under 5 h of calcination.

This study found that under 4 h of calcination, the average T60 values of clastic texture and transitional crystalline texture limestones were 26.4 s and 98.0 s, respectively. During the reaction of the crystalline BY sample with deionized water, the temperature threshold was lower than 60 °C; that is to say, the T60 value of the BY sample did not exist. Notably, the quicklime generated from the clastic-textured limestones had the highest

reaction activity. The PGX sample had the lowest T60 value (18.0 s) under 4 h of calcination, showing the highest quicklime reaction activity. The average T60 values of clastic texture, transitional crystalline texture, and crystalline texture of limestones were 26.9 s, 76.0 s, and 94.0 s under 5 h of calcination, respectively. Similarly, the clastic texture of limestones also showed the highest quicklime reaction activity. The XCC sample had the lowest T60 value (16.0 s), showing the highest quicklime reaction activity. Generally speaking, the limestones with a clastic texture had higher quicklime reaction activity than others during the same calcination time period. These results show that the quicklime produced by limestones with a clastic texture had a lower T60 value (high reaction activity) than that with other textures during the same calcination time period. The reasons are illustrated below.

(1) Limestone with a clastic texture is composed of granular calcite particles of different sizes and, therefore, has a relatively larger surface area and more internal channels. The calcined quicklime retains the original limestone characteristics, such as a large surface area and porous texture, which enhance the reaction activity. In contrast, limestone with a crystalline texture, particularly microcrystalline granular limestone, is composed of homogeneous crystalline grains. Therefore, its surface area is relatively small, its internal channels are relatively few, its structure is dense, and the calcined quicklime has low reaction activity. These results are also supported by the works of Moropoulou et al. (2001) and Yang et al. (2014), which state that limestone with a dense structure shows relatively lower quicklime reaction activity [31,32]. (2) The clastic texture is the loosest and most disordered. The disordered structure can be thought, thermodynamically, to have a higher initial entropy (S), which means that during the calcination process, limestone with a clastic texture is more prone to react and to increase in entropy value, and the calcined quicklime has a higher reaction activity and can react with water more easily. In contrast, the limestone with a crystalline texture has relatively ordered textures and a lower initial entropy and needs to overcome more entropy differences to react with water.

4.2. The Effect of Calcite Particle Size of Limestone on Quicklime Reaction Activity

The quicklime produced from limestone of a clastic texture has a higher reaction activity than that from limestone of other textures. Therefore, this study reveals the effect of calcite particle size on the quicklime reaction activity by comparing the reaction activity of calcined quicklime produced by limestone of the same clastic texture.

The relationship between the quicklime reaction activity and calcite particle size of limestone from Pingguo and Xincheng mines is shown in Figure 9.

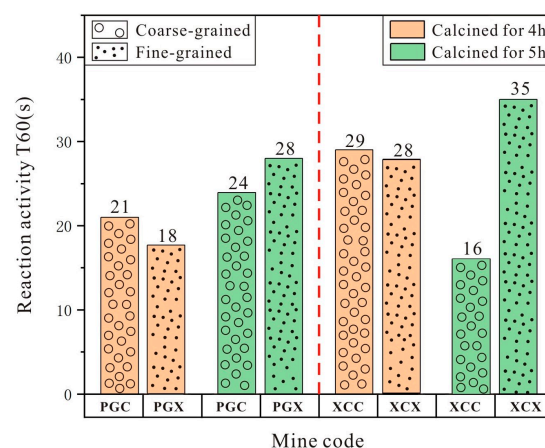


Figure 9. Comparison chart of the quicklime reaction activity of calcite of different particle sizes in clastic texture.

The T60 values of the quicklime produced under 4 h of calcination from Pingguo fine-grained limestone and coarse-grained limestone were 18.0 and 21.0 s, respectively (Table 3, Figure 9). The T60 value of the quicklime produced from fine-grained limestone was less

than that from coarse-grained limestone, which means the fine-grained limestone has a higher quicklime reaction activity. The T60 values of the quicklime produced under 4 h of calcination from Xincheng fine-grained limestone and coarse-grained limestone were 28.0 s and 29.0 s, respectively, also indicating that the T60 value of the quicklime from fine-grained limestone is less than that from coarse-grained limestone. Both examples show that the T60 values of the quicklime produced from fine-grained limestone are lower than those from coarse-grained limestones and indicate that under 4 h of calcination, the smaller the calcite particle is, the higher the quicklime reaction activity will be (Table 3).

The T60 values of the quicklime produced under 5 h of calcination from Pingguo fine-grained and coarse-grained limestones were 28.0 s and 24.0 s, respectively, which were higher than those under 4 h of calcination. The T60 values of the quicklime produced under 5 h of calcination from Xincheng fine-grained and coarse-grained limestones were 35.0 s and 16.0 s, respectively. The quicklime T60 values from the fine-grained limestones were higher, and the quicklime T60 values from the coarse-grained limestones were lower than those produced under 4 h of calcination.

The 10 μm particle size is used as a critical point. The PGC, PGX, XCX fine-grained limestones with calcite grain sizes of less than 10.0 μm were over-burnt under 5 h of calcination. The XCC limestone with a calcite grain size of more than 10.0 μm was under-burnt under 4 h of calcination.

The above phenomenon can be explained by using the decomposition model for spherical calcium carbonate [33]. The carbonate particles can be divided into three distinct layers, which are the sintered layer, the reacted layer, and the unreacted layer, during the calcination process (Figure 10). The outermost layer is also called the sintered layer, where CaCO_3 decomposes into CaO and a large amount of CO_2 is released during calcination. The surface of CaO crystallizes quickly at high temperatures and forms a dense layer. In the reacted layer, in the intermediate of the spherical calcium carbonate, CaO grains are not yet fully grown, and CO_2 release leads to the formation of numerous small pores. In the unreacted layer in the center of the spherical calcium carbonate, the temperature required for CaCO_3 decomposition is not fully up to standard; thus, CaCO_3 is only partially decomposed. The relatively fine-grained limestone possesses a larger surface area, more micro-pores, and faster heat transfer, which favors the quick decomposition of CaCO_3 during limestone calcination. The fine-grained limestone quickly finishes the decomposition reaction with a relatively shorter calcination time (4 h), and the produced quicklime is relatively more reactive. On the contrary, coarse-grained limestone cannot be completely decomposed with a short calcination time (4 h), and the produced quicklime is relatively less reactive. With the longer calcination time (5 h), the fine-grained limestone undergoes rapid development of CaO crystals on its surface, leading to the contraction of pores and the formation of a dense over-burnt layer. This layer thickens to the inner depth of the particles, and the generated quicklime has relatively lower reaction activity. This phenomenon is further verified in Tables 2 and 3. The calcination time of Pingguo coarse and fine limestone increased from 4 h to 5 h, and the T60 values of quicklime increased by 14% and 56%, respectively, which means the quicklime reaction activity decreased by 14% and 56%, respectively. The Pingguo fine-grained limestone was over-burnt after 5 h of calcination. On the contrary, the increase in calcination time led the heat to transfer to the unreacted layer inside the coarse-grained limestone. This allowed the internal CO_2 to escape, leading to an increase in micro-pores on the surfaces of the particles. As a result, heat could penetrate deeper into the particles, which facilitated the complete decomposition of CaCO_3 . This process yielded quicklime with a relatively higher reaction activity [34]. For Xincheng coarse-grained limestone, the increase in calcination time from 4 h to 5 h resulted in a decrease in the T60 value of quicklime by 45%, which means a 45% increase in the quicklime reaction activity, indicating that the heat provided under 4 h of calcination was not sufficient for CaCO_3 to decompose completely. The T60 value of the quicklime generated by Xincheng fine-grained limestone increased by 25%, which means a 25% decrease in the quicklime reaction activity. Similarly, with the Pingguo quicklime sample, over-burning occurred.

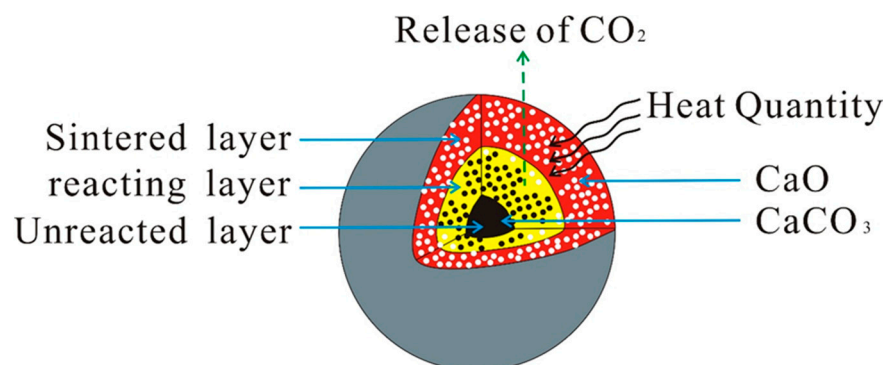


Figure 10. Schematic diagram of the decomposition model for spherical calcium carbonate.

In summary, with the same clastic texture, the relatively fine-grained limestone is much easier for CaCO_3 decomposition than the coarse-grained one during calcination and much easier to produce the same or more reactive quicklime with lower energy consumption.

5. Conclusions

This study explored the relationship between the natural physicochemical parameters of limestone and quicklime reaction activity, and the following conclusions can be drawn accordingly:

- (1) Compared with limestone with a crystalline texture (transitional crystalline texture included), limestone with a clastic texture is much easier to yield quicklime with a high reaction activity; and
- (2) With the same clastic texture, fine-grained limestone is much easier to yield a quicklime of high reaction activity than the coarse-grained one, and its energy consumption is also much lower.

Author Contributions: Conceptualization, J.W.; formal analysis, M.Z. and J.W.; validation, Z.Y.; investigation, M.Z. and Z.Y.; resources, Y.Z. and Q.R.; visualization, Q.W.; writing—original draft preparation, M.Z.; writing—review and editing, J.W.; supervision, Y.Z.; funding acquisition, J.W. All authors have read and agreed to the published version of the manuscript.

Funding: This project was financially supported by National Natural Science Foundation of China (NSFC: 42062007) and The Scientific Research Fund of Guangxi University, China (XGZ150264).

Data Availability Statement: All relevant data are available in the paper.

Acknowledgments: The Scientific Research Fund of Guangxi University, China and NSFC are acknowledged for funding this study. The anonymous reviewers are thanked for their thorough and detailed review of the manuscript. Guangxi Huana New Materials Co., Ltd. is thanked for providing experimental resources support for this study.

Conflicts of Interest: The authors declare no conflict of interest.

References

1. Kitamura, S. Dissolution behavior of lime into steelmaking slag. *Isij Int.* **2017**, *57*, 1670–1676. [[CrossRef](#)]
2. Yan, Z.M.; Li, Z.S.; Sanjeev, M.; Francois, P.; Sorinel, N. Value in use of lime in BOF steelmaking process. *Ironmak. Steelmak.* **2022**, *49*, 42–48.
3. Vola, G.; Bresciani, P.; Rodeghero, E.; Sarandrea, L.; Cruciani, G. Impact of rock fabric, thermal behavior, and carbonate decomposition kinetics on quicklime industrial production and slaking reactivity. *J. Therm. Anal. Calorim.* **2019**, *136*, 967–993. [[CrossRef](#)]
4. Madhav, D.; Buffel, B.; Desplentere, F.; Moldenaers, P.; Vandeginste, V. Bio-inspired mineralization of CO_2 into CaCO_3 : Single-step carbon capture and utilization with controlled crystallization. *Fuel* **2023**, *345*, 128157. [[CrossRef](#)]
5. Chu, S. Carbon capture and sequestration. *Science* **2009**, *325*, 1599. [[CrossRef](#)]
6. Yadav, S.; Mondal, S.S. A review on the progress and prospects of oxy-fuel carbon capture and sequestration (CCS) technology. *Fuel* **2022**, *308*, 122057. [[CrossRef](#)]

7. Gheevarthese, O.; Strydom, C.A.; Potgieter, J.H.; Potgieter, S.S. The influence of chloride and sulphate ions on the slaking rate of lime derived from different limestone deposits in South Africa. *Water SA* **2002**, *28*, 45–48. [[CrossRef](#)]
8. Rao, F.M.; Wu, Z.P.; Le, K.X. Calcination of active lime with small-sized limestone. *Met. Mine* **2007**, *2*, 88–90. (In Chinese)
9. Xue, Z.L.; Ke, C.; Liu, Q. Research on the reactivity of lime fast calcined at high temperature. *Steelmaking* **2011**, *27*, 37–40. (In Chinese)
10. Chen, H.; Zhang, S.H.; Yang, H.P.; Wang, X.H.; Chen, H.P. Activity analysis of limestone calcined product. *Inorg. Chem. Ind.* **2013**, *45*, 12–14. (In Chinese)
11. Ai, L.Q.; Zhang, X.M.; Zhang, Y.L. Lime activity and microstructure by microwave heating. *Iron Steel* **2015**, *50*, 76–80. (In Chinese)
12. Hao, H.Q.; Zhang, Y.Z.; Hao, S.J.; Zhang, C.F.; Jiang, W.F.; Gui, P.H. Preparation and metallurgical analysis of high activity burnt lime for steelmaking. *J. Iron Steel Res. Int.* **2016**, *23*, 884–890. [[CrossRef](#)]
13. Wang, X.Y.; Xue, Z.L.; Li, J.L. Research on the activity of limes calcinated using limestones with different properties at high temperature. *Steelmaking* **2016**, *32*, 73–78. (In Chinese)
14. Commandré, J.M.; Salvador, S.; Nzihou, A. Reactivity of laboratory and industrial limes. *Chem. Eng. Res. Des.* **2007**, *85*, 473–480. [[CrossRef](#)]
15. Potgieter, J.; Potgieter, S.; Moja, S.; Mulaba-Bafubandi, A. An empirical study of factors influencing lime slaking. Part I: Production and storage conditions. *Miner. Eng.* **2002**, *15*, 201–203. [[CrossRef](#)]
16. Wang, X.Y.; Xue, Z.L.; Li, J.L. Investigation of the reactivity and grain size of lime calcined at extra-high temperatures by flash heating. *J. S. Afr. Inst. Min. Metall.* **2016**, *116*, 1159–1164. [[CrossRef](#)]
17. Shin, H.G.; Kim, H.; Kim, Y.N.; Lee, H.S. Effect of reactivity of quick lime on the properties of hydrated lime sorbent for SO₂ removal. *J. Mater. Sci. Technol.* **2009**, *25*, 329.
18. Glasson, D.R. Reactivity of lime and related oxides. VIII. Production of activated lime and magnesia. *J. Appl. Chem.* **1963**, *13*, 111–119. [[CrossRef](#)]
19. Cai, J.; Xue, Z.; Hu, B.H.; Wang, L.Y.; Li, J.L. Research on the physico-chemical properties and microstructure of lime rapidly calcined at high temperature. *Steelmaking* **2017**, *33*, 43–48. (In Chinese)
20. Wang, L.; Xue, Z.; Cai, J.; Hu, B. Relationship between microstructure and properties of limestone calcined rapidly at high temperatures. *Trans. Indian Inst. Met.* **2019**, *72*, 3215–3222. [[CrossRef](#)]
21. Mou, Q.Q.; Li, J.L.; Zhang, M.X.; Zhu, R.L. Research on evolution behavior of the quick-lime reactivity under high temperature. *Steelmaking* **2020**, *36*, 79–84. (In Chinese)
22. Kantiranis, N.; Filippidis, A.; Christaras, B.; Tsirambides, A.; Kassoli-Fournaraki, A. The role of organic matter of carbonate rocks in the reactivity of the produced quicklime. *Mater. Struct.* **2003**, *36*, 135–138. [[CrossRef](#)]
23. Houngaloune, S.; Ariffin, K.S.; Hussin, H.B.; Watanabe, K.; Nhinxay, V. The effects of limestone characteristic, granulation and calcination temperature to the reactivity of quicklime. *Malays. J. Microsc.* **2010**, *6*, 53–57.
24. Elert, K.; Bel-Anzué, P.; Burgos-Ruiz, M. Influence of calcination temperature on hydration behavior, strength, and weathering resistance of traditional gypsum plaster. *Constr. Build. Mater.* **2023**, *367*, 130361. [[CrossRef](#)]
25. Mirzaei, H.; Noaparast, M.; Abdollahi, H. Modelling of limestone calcination for optimisation of prallel flow regenerative shaft kiln (PFR), case study: Iran Alumina Plant. *Arch. Min. Sci.* **2022**, *67*, 209–222.
26. Kılıç, Ö. The influence of high temperatures on limestone P-wave velocity and Schmidt hammer strength. *Int. J. Rock Mech. Min. Sci.* **2006**, *43*, 980–986. [[CrossRef](#)]
27. Chen, G.R. Effect of calcination of limestone on nano-sized calcium carbonate. *Inorg. Chem. Ind.* **2009**, *41*, 46–47. (In Chinese)
28. Kumar, G.S.; Ramakrishnan, A.; Hung, Y.T. Lime calcination. In *Advanced Physicochemical Treatment Technologies*; Humana Press: Totowa, NJ, USA, 2007; pp. 611–633.
29. Suleiman, I.E.; Abubakar, A.; Otuoze, H.S.; Suleiman, M.A.; Momoh, R.O.; Aliyu, S.N. Effects of particle size distribution on the burn ability of limestone. *Leonardo Electron. J. Pract. Technol.* **2013**, *12*, 115–130.
30. Gallala, W.; Gaied, M.E.; Tlili, A.; Montacer, M. Factors influencing the reactivity of quicklime. *Proc. Inst. Civ. Eng.-Constr. Mater.* **2008**, *161*, 25–30. [[CrossRef](#)]
31. Moropoulou, A.; Bakolas, A.; Aggelakopoulou, E. The effects of limestone characteristics and calcination temperature to the reactivity of the quicklime. *Cem. Concr. Res.* **2001**, *31*, 633–639. [[CrossRef](#)]
32. Yang, Y.J.; Jegal, Y.J.; Nam, S.Y.; Kim, J.; Ahn, J.W. An exploratory research on PCC application of crystalline limestone: Effects of limestone crystallographic characteristics on hydraulic activity. *J. Korean Ceram. Soc.* **2014**, *51*, 115–120. [[CrossRef](#)]
33. Milne, C.R.; Silcox, G.D.; Pershing, D.W.; Kirchgessner, D.A. Calcination and sintering models for application to high-temperature, short-time sulfation of calcium-based sorbents. *Ind. Eng. Chem. Res.* **1990**, *29*, 139–149. [[CrossRef](#)]
34. Zhang, K.; Wang, S.; Li, C.; Sun, H.; Zhang, Y. Decomposition Mechanism and Calcination Properties of Small-Sized Limestone at Steelmaking Temperature. *Processes* **2023**, *11*, 1008. [[CrossRef](#)]

Disclaimer/Publisher's Note: The statements, opinions and data contained in all publications are solely those of the individual author(s) and contributor(s) and not of MDPI and/or the editor(s). MDPI and/or the editor(s) disclaim responsibility for any injury to people or property resulting from any ideas, methods, instructions or products referred to in the content.